



HAL
open science

The valence shell electronic states of trimethylene oxide studied by photoabsorption and ab initio multireference interaction calculations

David Michael Holland, Isobel Walker, David Shaw, Ian Mcewen, Martyn Guest

► To cite this version:

David Michael Holland, Isobel Walker, David Shaw, Ian Mcewen, Martyn Guest. The valence shell electronic states of trimethylene oxide studied by photoabsorption and ab initio multireference interaction calculations. *Molecular Physics*, 2009, 107 (14), pp.1473-1483. 10.1080/00268970902946368 . hal-00513290

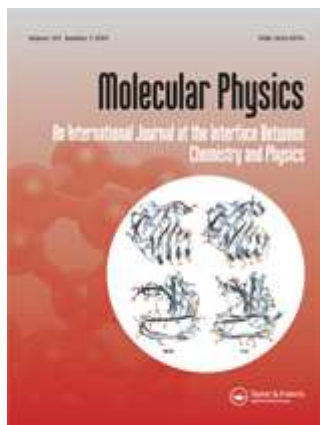
HAL Id: hal-00513290

<https://hal.science/hal-00513290>

Submitted on 1 Sep 2010

HAL is a multi-disciplinary open access archive for the deposit and dissemination of scientific research documents, whether they are published or not. The documents may come from teaching and research institutions in France or abroad, or from public or private research centers.

L'archive ouverte pluridisciplinaire **HAL**, est destinée au dépôt et à la diffusion de documents scientifiques de niveau recherche, publiés ou non, émanant des établissements d'enseignement et de recherche français ou étrangers, des laboratoires publics ou privés.



The valence shell electronic states of trimethylene oxide studied by photoabsorption and ab initio multireference interaction calculations

Journal:	<i>Molecular Physics</i>
Manuscript ID:	TMPH-2009-0082.R1
Manuscript Type:	Full Paper
Date Submitted by the Author:	30-Mar-2009
Complete List of Authors:	Holland, David; Daresbury Laboratory, Photon Science Walker, Isobel; Heriot-Watt University Shaw, David; Daresbury Laboratory McEwen, Ian; Heriot-Watt University Guest, Martyn; University of Cardiff
Keywords:	photoabsorption, configuration interaction, Rydberg states, trimethylene oxide



1
2
3
4 **The valence shell electronic states of trimethylene oxide studied by photoabsorption and**
5 **ab initio multireference configuration interaction calculations**
6
7
8
9

10
11
12 I.C. WALKER¹, D.M.P. HOLLAND², D.A. SHAW², I.J. McEWEN¹ and M.F. GUEST³
13
14

15
16 ¹School of Engineering and Physical Sciences, Heriot-Watt University, Riccarton, Edinburgh
17
18 EH14 4AS, UK
19

20 ²Daresbury Laboratory, Daresbury, Warrington, Cheshire WA4 4AD, UK
21

22 ³Advanced Research Computing, Cardiff University, Redwood Building, King Edward VII
23
24 Avenue, Cardiff CF10 3NF, UK
25
26
27
28
29

30
31 The absolute photoabsorption cross section of trimethylene oxide has been measured between
32 threshold and 30 eV using monochromated synchrotron radiation. Below the ionization
33 threshold the spectrum exhibits numerous sharp peaks associated with Rydberg states
34 belonging to series converging onto the \tilde{X}^2B_1 limit. At excitation energies above the
35 ionization threshold at 9.680 eV intravalence transitions play a dominant role, resulting in the
36 appearance of prominent broad bands. Ab initio multireference configuration interaction
37 calculations have been performed to obtain excitation energies for valence electron
38 transitions into Rydberg or virtual valence orbitals. These theoretical predictions have
39 enabled assignments to be proposed for most of the structure due to Rydberg series
40 converging onto the \tilde{X}^2B_1 limit. The calculations show that configuration interaction is
41 important in the description of some of the excited states. The photoabsorption spectrum of
42 trimethylene oxide has been compared with those of ethylene oxide, ethylene sulphide and
43 trimethylene sulphide to identify and characterize the principal Rydberg excitations that these
44 related three- or four-membered ring molecules have in common.
45
46
47
48
49
50
51
52
53
54
55
56
57
58
59
60

1. Introduction

The work reported here relates to combined experimental and theoretical studies on the electronic states of trimethylene oxide (also known as oxetane). The main experimental component is measurement of absolute photoabsorption cross sections between threshold and 30 eV, using synchrotron radiation. We have also obtained accurate ionization energies by recording a threshold photoelectron spectrum. The experimental data are interpreted using the results of *ab initio* multireference calculations. As well as assisting in spectral assignments, these computations have given insight into configuration interaction and the mixing of Rydberg and valence orbitals [1-3].

Trimethylene oxide is a four-membered cyclic ether (C_3H_6O) related to cyclobutane (C_4H_8) by substitution of an oxygen atom for one of the methylene (CH_2) groups. Like ethylene oxide (C_2H_4O), which is the corresponding three-membered ring compound, trimethylene oxide and its derivatives are reactive, a consequence of ring strain. Trimethylene oxide, unlike ethylene oxide, can relieve some of this strain by adopting a puckered rather than a planar ring structure. Consequently, in the ground electronic state the molecule oscillates between two equivalent bent conformers in a ring puckering vibration of small amplitude. The origin of this vibrational band lies at 52.92 cm^{-1} (6.56 meV) [4]. However, the molecule is unusual in that the potential barrier at the planar configuration is so small (15.52 cm^{-1} , 1.92 meV) that the zero level of the puckering vibration is 11.86 cm^{-1} (1.47 meV) *above* the barrier [5-7]. The molecule is therefore essentially planar and of C_{2v} symmetry.

Oxetanes are important monomers in the production of resistant resins and films and are valuable reagents in the preparation of larger heterocyclic molecules. The oxetane ring is an essential component of a number of biologically active molecules. There are thus both pure and applied reasons for exploring the electronic structure of this class of compound. The present work follows from similar studies on other small-ring systems, namely cyclopropane[8], ethylene oxide [9], ethylene sulphide [10] and trimethylene sulphide [11].

1
2
3
4 Assuming C_{2v} symmetry, and with the molecule lying in the yz plane, the ground state
5
6 electronic configuration is, from the present work:-

7
8 core: $(1a_1)^2(2a_1)^2(1b_2)^2(3a_1)^2$

9
10 valence: $(4a_1)^2(5a_1)^2(2b_2)^2(6a_1)^2(1b_1)^2(7a_1)^2(3b_2)^2(1a_2)^2(2b_1)^2(4b_2)^2(8a_1)^2(3b_1)^2$

11
12 The highest occupied molecular orbital, $3b_1$, is effectively a π , non-bonding orbital centred on
13
14 the O atom. Orbitals of symmetry a_2 are also π -type while a_1 and b_2 are σ -type. (Some
15
16 earlier workers made the molecular plane xz in which case the b_1 and b_2 symmetries are
17
18 interchanged).
19

20
21
22 HeI excited photoelectron spectra have been reported by Mollere [12], Mollere and Houk
23
24 [13] and Roszak et al [14]. Only the $(3b_1)^{-1} \tilde{X}^2B_1$ state photoelectron band shows
25
26 vibrational structure in a short progression with a spacing of about 150 meV. There are
27
28 differences between reported ionization energies; in order to resolve these, we have recorded
29
30 a threshold photoelectron spectrum.
31

32
33
34 An early photoabsorption spectrum of trimethylene oxide, spanning about 6.2–8 eV, was
35
36 obtained by Fleming et al [15]. Hernandez [16] extended the spectral range; he identified a
37
38 relatively long d-type Rydberg series which is confirmed in the present work.
39

40 41 2. Experimental apparatus and procedure

42
43 The absolute photoabsorption cross section of trimethylene oxide was measured using two
44
45 experimental chambers – a cell incorporating LiF windows [10], and a double ion chamber
46
47 [17] – and synchrotron radiation emitted from the Daresbury Laboratory storage ring. In both
48
49 cases the experimental chamber was attached to a 5m normal incidence monochromator,
50
51 which delivers radiation over the photon energy range of 5-40 eV, and has been described
52
53 previously [18]. In the present experiment a photon resolution of 0.1 nm FWHM (~ 5 meV at
54
55 $h\nu = 8$ eV) was employed.
56

57
58 Each of the LiF windows defining the absorption cell was mounted in a gate valve, with the
59
60 distance between the windows being 25.6 cm. After passing through the second of these

1
2
3
4 windows, the radiation entered an evacuated region, before impinging upon a sodium
5 salicylate screen sprayed onto a glass window. The resulting fluorescence was detected with
6 a photomultiplier. The gas pressure was measured using a 0-1 Torr capacitance manometer.
7
8
9

10
11 The absolute photoabsorption cross section was obtained through application of the Beer-
12 Lambert law, $I_t = I_o \exp(-n\sigma l)$, where I_t is the intensity of the transmitted radiation after
13 passing through the gas column, I_o is the corresponding incident intensity, n is the gas
14 number density, σ is the photoabsorption cross section and l is the length of the gas column.
15 To determine σ as a function of photon energy, the monochromator was stepped over the
16 chosen energy range and at each step readings proportional to I_t and the electron beam current
17 in the storage ring were recorded. The pressure was also read. The entire procedure was then
18 repeated with the cell empty to obtain I_o . Photoabsorption spectra were recorded using gas
19 pressures in the 5-30 μ bar range. The experimental uncertainty associated with the
20 determination of absolute photoabsorption cross sections using this cell is estimated as ~5%.
21
22
23
24
25
26
27
28
29
30
31
32
33

34 To calibrate the photon energy scale, high resolution absorption spectra of a gas mixture
35 comprising trimethylene oxide, nitrous oxide and nitric oxide were recorded. As the spectra
36 of nitrous oxide and nitric oxide contain many sharp peaks of well established photon energy,
37 this procedure enabled the energy scale of the spectrum of trimethylene oxide to be
38 calibrated.
39
40
41
42
43
44

45 At higher photon energies, the absolute photoabsorption cross section was measured using a
46 double ion chamber [17]. This chamber incorporates a set of plates, two of which were used
47 to collect the photoions. A photoabsorption spectrum of trimethylene oxide was measured by
48 stepping the monochromator over the desired photon energy range, and recording two
49 electrometer currents and the gas pressure. The photon energy scale was calibrated by
50 recording high resolution absorption spectra of a gas mixture comprising trimethylene oxide,
51 argon and xenon.
52
53
54
55
56
57
58
59
60

1
2
3
4 The threshold photoelectron spectrum was recorded using only the electron side of a
5 threshold photoelectron-photoion coincidence spectrometer [19] attached to the 5m normal
6 incidence monochromator. In the spectrometer source region the monochromatic photon
7 beam interacts with an effusive beam of the gas under investigation, and a small electric field
8 is used to extract threshold (zero kinetic energy) electrons formed through photoionization.
9 The detection system consists of a lens optimized for high transmission of low energy
10 electrons, followed by a hemispherical electrostatic analyser. After passing through the
11 interaction region the incident radiation impinges upon a sodium salicylate coated screen and
12 the resulting fluorescence was detected with a photomultiplier. This signal was used for
13 normalization purposes. The threshold photoelectron spectrum of trimethylene oxide was
14 measured at an overall resolution of ~10 meV FWHM. The photon energy scale was
15 calibrated by recording a threshold photoelectron spectrum of a gas mixture comprising
16 trimethylene oxide, argon and xenon.
17
18
19
20
21
22
23
24
25
26
27
28
29
30
31

3. Computational details

32
33 The present theoretical study investigates the vertical excitation energies for the
34 electronically excited singlet transitions of trimethylene oxide in the 0-15 eV region. The
35 nature of the electronic state as valence or Rydberg is established by means of the second
36 moments of the electronic charge distribution ($\langle x^2 \rangle$ etc). The ab initio methods used were
37 from the GAMESS-UK suites of programs [20,21], and all excited state calculations
38 employed the multireference double excitation configuration interaction (MRDCI) method.
39 The (semi-) direct version of the MRDCI module is due to Engels et al [22] and Krebs and
40 Buenker [23], and is derived from the original table-driven implementation [24].
41
42
43
44
45
46
47
48
49
50
51

52 The geometry of trimethylene oxide was fully optimised at the MP2 level using both cc-
53 pVTZ and cc-pVDZ basis sets [25-28]. The vertical excitation energy study was performed
54 at the cc-pVTZ optimised equilibrium geometry using the cc-pVDZ basis set augmented with
55 additional diffuse s-, p- and d-type functions (2s, 2p and 2d) which are placed at the oxygen
56 atom [29]. All the MRDCI calculations were performed in C_{2v} symmetry, and resulted in the
57 ground state electronic configuration given in the Introduction. The lowest lying unoccupied
58
59
60

1
2
3
4 orbitals are computed to be of Rydberg type, namely $3s_{a_1}$, $3p_{b_2}$, $3p_{b_1}$, $3p_{a_1}$, $3d_{a_1}$, $3d_{b_2}$, $3d_{b_1}$,
5
6 $3d_{a_2}$, $3d_{a_1}$, ... followed by valence orbitals $8b_1$, $17a_1$, $18a_1$, $4a_2$, $9b_2$, $19a_1$, $10b_2$, $9b_1$, ...
7
8

9
10 In the CI calculations, the core and inner shell orbitals are frozen with double occupancy,
11 while the virtual molecular orbital set varied from 70 to 90 orbitals. The MRDCI
12 diagonalization stage contained a reference set range of configuration state functions (CSF)
13 ~35, which expanded to ~40 CSF when spin combinations of four-open-shell CSF were
14 considered. Up to 27 roots of each symmetry were determined simultaneously. The
15 calculated excitation energies for transitions originating in the occupied valence shell orbitals
16 are listed in table 1 (valence states) and table 2 (Rydberg states). The oscillator strengths
17 have been calculated using both the dipole length ($f(r)$) and the dipole velocity ($f(\nabla)$)
18 formulas [30]. These expressions must yield the same results when exact electronic
19 wavefunctions are employed in the calculations, but it has been argued [31,32] that the length
20 form will generally (but not always) provide more reliable results when approximate
21 wavefunctions are used. Thus, the results reported in the present work were obtained using
22 the dipole length formulation. Only transitions whose oscillator strengths ($f(r)$) are greater
23 than ~0.001 are included in the tables, except for some low-lying electric-dipole forbidden
24 transitions.
25
26
27
28
29
30
31
32
33
34
35
36
37
38
39
40

41
42 The vertical ionization energies and their relative spectral intensities (pole strengths) were
43 obtained using the Outer Valence Green's Function (OVGF) approach [33]. The results are
44 listed in table 3, together with charge distribution analyses. These analyses show that, of the
45 $n=3$ Rydberg orbitals, all except two ($3d_{a_1}$ and $3d_{a_2}$) have mixed l character (where l is the
46 orbital angular momentum) so that strong configuration interaction can be expected in the
47 Rydberg states. A similar behaviour was observed for the related molecules ethylene oxide
48 [9], ethylene sulphide [10] and trimethylene sulphide [11].
49
50
51
52
53
54
55
56
57
58
59
60

4. Results and discussion

4.1. Threshold photoelectron spectrum

The threshold photoelectron spectrum of trimethylene oxide is plotted in figure 1 and is generally similar to the HeI excited spectrum [12-14]. The results from the OVGf calculations show that the single particle model of ionization [34] holds for all the valence orbitals apart from the most tightly bound $5a_1$ and $4a_1$ orbitals. The spectrum also closely resembles that of trimethylene sulphide although the ordering of the $1a_2$ and $3b_2$ orbitals is reversed. The theoretical vertical ionization energies (table 3) are in good agreement with the experimental values (table 4), thereby allowing the photoelectron bands to be associated with ionization from specific molecular orbitals. The band due to the $6a_1$ orbital exhibits a doublet, with maxima at 18.74 and 19.01 eV. This suggests that electron correlation is spreading the intensity associated with the main line amongst several satellite states.

As in the HeI excited spectrum of trimethylene oxide [12-14], only the $(3b_1)^{-1} \tilde{X}^2B_1$ state band in the threshold photoelectron spectrum exhibits vibrational structure. Previous analyses have attributed this structure to excitation of a single vibrational mode. The binding energies of the first two peaks, at 9.679 and 9.833 eV, result in a splitting of 154 meV. Assuming that this spacing is due to one of the totally symmetric vibrational modes, the most likely is ν_5^+ , a CH_2 wag, whose energy in the molecular ground state is 166.5 meV [35]. However, a more detailed inspection of the threshold photoelectron spectrum reveals that the peaks at ~10.0 and 10.15 eV are doublets. Moreover, an assignment in terms of a single progression in the ν_5^+ mode leads to an irregular anharmonicity. Thus, it appears that the vibrational structure should be ascribed to two progressions, each involving the ν_5^+ mode, with one of the progressions having an additional excitation of another mode whose energy is ~335 meV. Since the ν_1 and ν_2 modes (both C-H stretch) have similar energies, of ~365 meV, in the molecular ground state [35], it is probable that the second progression in the \tilde{X}^2B_1 state photoelectron band involves a single quantum of one of these modes.

Although the vertical ionization energies (table 4) derived from the peaks in the threshold photoelectron spectrum are similar to those obtained from the HeI excited spectrum [12-14],

1
2
3
4 the relative intensities of the corresponding peaks are not necessarily the same. These
5 differences are particularly evident in the binding energy range ~11-16 eV, which
6 encompasses the bands associated with the $8a_1$, $4b_2$, $2b_1$, $1a_2$ and $3b_2$ orbitals, and arise
7 because the signal in a conventional electron energy resolved spectrum is dominated by direct
8 transitions, whereas resonant autoionization may contribute substantially to the signal in a
9 threshold photoelectron spectrum.
10
11
12
13
14
15
16
17

18 These relative intensity variations in the HeI excited and threshold photoelectron spectra of
19 trimethylene oxide are typical of those observed in small polyatomic molecules [36,37].
20 Experimentally it has been found that the relative intensities of photoelectron bands
21 associated with weakly bound orbitals tend to be greater in conventional spectra than in
22 threshold photoelectron spectra, whereas the converse holds for the more tightly bound
23 orbitals. The enhancement in the latter bands can be attributed to resonant autoionization
24 from numerous superexcited (Rydberg or valence) states.
25
26
27
28
29
30
31
32
33

34 4.2. Photoabsorption spectrum

35 4.2.1. Valence states

36
37 The present calculations predict that intravalence transitions out of the three highest occupied
38 orbitals ($3b_1$, $8a_1$ and $4b_2$) occur between about 9.5 and 14 eV. That is, the first of the
39 valence-excited states lies close to the ionization threshold (9.680 eV). Only the first four
40 optically-allowed intravalence transitions, which have a common receiving orbital, $17a_1$ (σ^*),
41 and some Rydberg character, have positive term values. The remainder, whose term values
42 are negative, lie *above* the ionization energy of the promoted electron and hence are expected
43 to give rise to very broad absorption bands, as is observed above about 10 eV (figure 2).
44 From the computed excitation energies, and considering calculated term values together with
45 measured ionization energies, we offer the following spectral assignments. Transitions
46 $3b_1 \rightarrow 17a_1$ and $4b_2 \rightarrow 17a_1$ contribute to the rise in the absorption cross section above about 9.5
47 eV. The maximum in the cross section at about 10.7 eV is, mainly, from $8a_1 \rightarrow 17a_1$ with
48 contributions from $4b_2 \rightarrow 17a_1$ and $3b_1 \rightarrow 8b_1$. The calculated excitation energy for the
49 transition $3b_1 \rightarrow 4a_2$ is close to that of the peak at 11.34 eV. The cross section goes through a
50
51
52
53
54
55
56
57
58
59
60
09-010

1
2
3
4 global maximum at 13.72 eV but the calculations do not extend sufficiently high in energy to
5
6 give a good account of this region. However, from the available data, most of the intensity
7
8 may be attributed to valence transitions, including $4b_2 \rightarrow 10b_2$ and $8a_1 \rightarrow 18a_1$.
9

10
11 Above the ionization threshold, broad overlapping bands, due to intravalence transitions,
12
13 dominate the photoabsorption cross section of trimethylene oxide and contributions from
14
15 Rydberg excitations are weak. A similar behaviour is observed in ethylene oxide [9],
16
17 ethylene sulphide [10] and trimethylene sulphide [11]. In each of these molecules an intense
18
19 structureless peak, which appears to share a common origin, occurs between 12 and 13 eV,
20
21 and is followed by a very broad maximum around 18 eV. The experimental data demonstrate
22
23 that a proper understanding of the valence shell photoabsorption spectra of these molecules
24
25 requires a theoretical study of the intravalence transitions up to an excitation energy of at
26
27 least 20 eV.
28
29

30 31 32 4.2.2. Rydberg states

33
34 It follows, from the computed valence-state energies and the photoelectron spectrum that,
35
36 below about 9.5 eV, (i) electronically-excited states are Rydberg in nature and (ii) vibrational
37
38 structure in the photoabsorption spectrum relates to excitation of Rydberg states converging
39
40 on the $(3b)^{-1}$ ionization energy at 9.680 eV. Of these Rydberg series, one s-type (symmetry
41
42 A_1), two p-type (A_1 and B_1) and four d-type (A_1 , $2xB_1$ and B_2) are electric-dipole allowed.
43
44

45
46 In making assignments (table 5), we consider the above aspects as well as the computed data
47
48 for Rydberg states. From its term value (3.06 eV) the first band, which shows absorption
49
50 peaks at 6.615 and 6.751 eV, can be assigned to the lowest-lying Rydberg state, namely $3b_13s$
51
52 (figure 3). However, the band profile demonstrates that the excited state is not purely
53
54 Rydberg. Taking a pragmatic approach, one could view the band as comprising the Rydberg
55
56 $3b_13s$ state sitting on a continuum provided by a dissociative (σ^*) valence state. However,
57
58 the computations produce a single excited state, predominately Rydberg, but including a
59
60 valence (σ^*) configuration in the upper state. The oscillator strength of this transition is
under-estimated in the calculations.

1
2
3
4 The origins of the two allowed $3b_1 \rightarrow 3p$ transitions fall at 7.111 eV and 7.654 eV. For the
5 first of these (assigned $3b_1 \rightarrow 3p_{a_1} B_1$) the vibrational structure matches that of the $\tilde{X}^2 B_1$ state
6 band in the threshold photoelectron spectrum (figure 1), confirming its Rydberg nature. The
7 band profile of the second allowed 3p state ($3b_1 \rightarrow 3p_{b_1} A_1$) is different in that each of the
8 broad vibration peaks is split by about 14 meV. Furthermore, such splitting pervades the
9 Rydberg states which dominate the remainder of the spectrum. We ascribe it to excitation of
10 (for reasons of symmetry) two quanta of the (b_1) ring puckering vibration, ν'_{18} . The
11 computations offer a reason for the absence of this vibration from the first of the 3p bands,
12 finding a valence component to the upper state which, we propose, reduces its lifetime and so
13 quenches the low-frequency vibration. The third $3b_1 3p$ state is of A_2 symmetry and hence
14 forbidden. Although it is computed to be the middle of the 3p components, it may be
15 responsible for weak structure at the high energy end of the 7.654 eV band, having gained
16 intensity through vibronic coupling.
17
18
19
20
21
22
23
24
25
26
27
28
29
30
31

32 The dominant Rydberg series in the spectrum is d-type having its first member at 8.048 eV
33 (8.39 eV calculated); on intensity grounds, we assign it to the electric-dipole-allowed B_2
34 ($3b_1 \rightarrow nd_{a_2}$) series (figures 4 and 5). Tabulated energies (table 5) for this long series are close
35 to those given by Hernandez [16]; energies for higher members should be taken as indicative
36 only. Origins at 7.957 eV and, tentatively, 8.070 eV are attributed to excitation of the two 3d
37 states of B_1 symmetry.
38
39
40
41
42
43
44
45

46 The appearance of the puckering vibration in the bands of pure Rydberg states indicates that
47 the dihedral angle in the ground state is slightly different to those in the excited states.
48 Probably the excited states (and the $\tilde{X}^2 B_1$ state) are planar.
49
50
51
52

53 Rydberg states associated with promotion of an electron from the orbital $8a_1$ will contribute
54 structureless bands above about 8.5 eV. The computed energy for the first of these, which is
55 of mixed s/p/d character, is 8.93 eV and may relate to the weak peak at 8.475 eV. Broad
56 bands visible on the rising side of some higher peaks may also originate in transitions out of
57 the $8a_1$ orbital. Similar broad bands below the $8a_1$ excitation threshold (at, for example,
58
59
60

1
2
3
4 ~8.003, 8.017 and 8.030 eV) remain to be accounted for. We propose that these are hot
5
6 bands. In making tentative assignments of hot bands (table 5), we have used ground-state
7
8 vibrational spacings for the puckering mode, ν_{18} , given by Winnewisser et al [4]; these are
9
10 $\nu_0^1 = 6.56$, $\nu_1^2 = 11.10$, $\nu_2^3 = 12.95$, $\nu_3^4 = 14.62$ meV. Confirmation of hot bands will require
11
12 further experimental work, such as absorption measurements at different temperatures.
13
14

15
16 Rydberg states calculated to contribute to the absorption intensity above the ionization
17
18 threshold may be extracted from table 2. The dominant states involve electron promotions
19
20 out of the $4b_2$, $2b_1$ or $1a_2$ orbitals but, in the absence of vibrational structure, it is not possible
21
22 to make specific assignments.
23
24

25 26 4.2.3. Summary of the electronic states due to Rydberg series in C_2H_4O , C_2H_4S , C_3H_6O and 27 28 C_3H_6S 29

30 In this, our concluding article on the valence shell electronic structure of the related three- or
31
32 four-membered ring molecules ethylene oxide [9], ethylene sulphide [10], trimethylene
33
34 sulphide [11] and trimethylene oxide (present work), we provide a summary of the principal
35
36 Rydberg states associated with series converging onto the ionization threshold \tilde{X}^2B_1 . The
37
38 relevant portions of the photoabsorption cross section are plotted in figure 6 and the
39
40 correlation amongst the related structure is indicated with dotted lines.
41
42

43
44 The calculations predict that the first absorption band with significant intensity should be
45
46 associated primarily with the $3sa_1/4sa_1 B_1$ state, although in the sulphur containing molecules
47
48 the $4pa_1 B_1$ state also contributes. In addition, in trimethylene oxide and sulphide an
49
50 intravalence transition occurs at a similar excitation energy. Configuration interaction
51
52 amongst these excited states results in a highly perturbed absorption band, due to both
53
54 Rydberg/Rydberg and Rydberg/valence mixing, exhibiting irregular structure.
55
56

57
58 The next feature that the molecules have in common is a band due to a transition into a p-type
59
60 Rydberg orbital. According to the theoretical studies, the state corresponds to $3pa_1 B_1$ in the

1
2
3
4 oxides and $4p_{a_1} A_1$ in the sulphides. In each case the absorption band displays regular
5
6 vibrational structure which resembles that in the $\tilde{X}^2 B_1$ state photoelectron band.
7
8

9
10 There follows a heavily congested region of the spectrum, due to transitions into various 3d
11
12 states and higher members of the p series, in which structure associated with Rydberg series
13
14 is difficult to recognise without theoretical guidance. The calculations demonstrate that
15
16 configuration interaction is strong and that this results in complex absorption bands which
17
18 cannot be ascribed to a single electronic configuration. At higher energies two extended
19
20 Rydberg series, with quantum defects of ~ 0.05 and 0.3 , emerge. The intense absorption
21
22 bands associated with these series dominate the spectrum. This is particularly evident in
23
24 trimethylene oxide. According to the calculations, the Rydberg series with $\delta \sim 0.3$
25
26 corresponds to $nda_1 B_1$ excitations in each molecule. The assignments for the Rydberg series
27
28 with $\delta \sim 0.05$ are more complicated. The predictions indicate that in the sulphides the series
29
30 correspond to $ndb_1 A_1$. However, in ethylene oxide the theoretical results suggest that the
31
32 series should be attributed to the second $nda_1 B_1$ series, whilst in trimethylene oxide the series
33
34 should be associated with $nda_2 B_2$ excitations. Thus, the calculations predict differing upper
35
36 states for the Rydberg series having $\delta \sim 0.05$.
37
38

39
40 Although we have been unable to assign all the structure due to Rydberg transitions from the
41
42 outermost orbital, our combined experimental and theoretical studies have enabled substantial
43
44 progress to be made in the understanding of the valence shell electronic states. The major
45
46 role played by configuration interaction in the description of the excited states has been
47
48 predicted and observed.
49

50 51 52 **5. Concluding remarks**

53
54 Robin [3] has written "...the alkyl ethers show an undeviating pattern of $n_0 3s, 3p, 3d$ bands
55
56 in the vacuum ultraviolet..." This statement, in general terms, applies to trimethylene oxide
57
58 for which Rydberg states may be identified using the photoelectron spectrum and the
59
60 Rydberg expression. However, the theoretical work shows that few of the low-lying Rydberg
states can be described by a single electronic configuration. Both Rydberg/Rydberg and

1
2
3
4 Rydberg/valence mixing occur. In the latter case, the intruding valence orbital ($17a_1$) is an
5
6 antibonding (σ) orbital. It mixes, first, with the $3s_{a_1}$ orbital giving valence (dissociative)
7
8 character to the (nominal) $3b_13s$ excited state. Also, the computations find that it contributes
9
10 to the upper configuration of the (nominal) $3b_13pa_1$ Rydberg state. In this case, we suggest,
11
12 the effect is to reduce the lifetime of the excited state, thereby eliminating the low-frequency
13
14 ring-puckering vibration which is active in the higher Rydberg states.
15
16

17
18 The Rydberg behaviour observed in trimethylene oxide resembles that in the three-membered
19
20 ring ether, ethylene oxide [9]. However, the valence patterns are different. In ethylene oxide,
21
22 the lowest-lying valence state (transition $2b_1 \rightarrow 8b_2$, computed term value 1.9) is electric-
23
24 dipole forbidden and it does not seem to affect the absorption spectrum. There appears to be
25
26 no involvement of valence configurations in Rydberg states, although Rydberg/Rydberg
27
28 mixing is widespread. On the other hand, Rydberg/valence mixing is evident in trimethylene
29
30 sulphide [11].
31
32

33
34 The authors are grateful for financial support from the Central Laboratory of the Research
35
36 Councils.
37
38
39
40
41
42
43
44
45
46
47
48
49
50
51
52
53
54
55
56
57
58
59
60

References

- [1] ROBIN, M.B., 1974, Higher excited states of polyatomic molecules. Vol 1 (New York: Academic Press).
- [2] ROBIN, M.B., 1975, Higher excited states of polyatomic molecules. Vol 2 (New York: Academic Press).
- [3] ROBIN, M.B., 1985, Higher excited states of polyatomic molecules. Vol 3 (Orlando: Academic Press).
- [4] WINNEWISSER, M., KUNZMANN, M., LOCK, M., and WINNEWISSER, B.P., 2001, *J. molec. Struct.*, **561**, 1.
- [5] CHAN, S.I., ZINN, J., and GWINN, W.D., 1961, *J. chem. Phys.*, **34**, 1319.
- [6] JOKISAARI, J., and KAUPPINEN, J., 1973, *J. chem. Phys.*, **59**, 2260.
- [7] LISTER, D.G., CHARRO, M.E., LOPEZ, J.C., ALONSO, J.L., EGGIMANN, T., and WIESER, H., 1993, *Chem. Phys.*, **172**, 303.
- [8] WALKER, I.C., HOLLAND, D.M.P., SHAW, D.A., McEWEN, I.J., and GUEST, M.F., 2007, *J. Phys. B*, **40**, 1875.
- [9] WALKER, I.C., HOLLAND, D.M.P., SHAW, D.A., McEWEN, I.J., and GUEST, M.F., 2008, *J. Phys. B*, **41**, 115101.
- [10] HOLLAND, D.M.P., SHAW, D.A., WALKER, I.C., McEWEN, I.J., and GUEST, M.F., 2008, *Chem. Phys.*, **344**, 227.
- [11] HOLLAND, D.M.P., SHAW, D.A., WALKER, I.C., McEWEN, I.J., and GUEST, M.F., 2009, *J. Phys. B*, **42**, 035102 (2009).
- [12] MOLLERE, P.D., 1973, *Tetrahedron Lett.*, **29**, 2791.
- [13] MOLLERE, P.D., and HOUK, K.N., 1977, *J. Amer. chem. Soc.*, **99**, 3226.
- [14] ROSZAK, S., KAUFMAN, J.J., KOSKI, W.S., BARRETO, R.D., FEHLNER, T.P., and BALASUBRAMANIAN, K., 1992, *J. phys. Chem.*, **96**, 7226.
- [15] FLEMING, G., ANDERSON, M.M. HARRISON, A.J., and PICKETT, L.W., 1959, *J. chem. Phys.*, **30**, 351.
- [16] HERNANDEZ, G.J., 1963, *J. chem. Phys.* **38**, 2233.

- 1
2
3
4 [17] SHAW, D.A., HOLLAND D.M.P., MacDONALD, M.A., HOPKIRK, A., HAYES,
5 M.A., and McSWEENEY, S.M., 1992, Chem. Phys., **163**, 387.
6
7
8 [18] HOLLAND, D.M.P., WEST, J.B., MacDOWELL, A.A., MUNRO, I.H., and
9 BECKETT, A.G., 1989, Nucl. Instrum. Methods B., **44**, 233.
10
11 [19] HOLLAND D.M.P., SHAW, D.A., SUMNER, I., HAYES, M.A., MACKIE, R.A.,
12 WANNBERG, B., SHPINKOVA, L.G., RENNIE, E.E., COOPER, L., JOHNSON,
13 C.A.F., and PARKER, J.E., 2001, Nucl. Instrum. Methods B., **179**, 436.
14
15 [20] GUEST, M.F., THOMAS, J.M.H., SHERWOOD, P., BUSH, I.J., VAN DAM, H.J.J.,
16 VAN LENTHE, H., HAVENITH, R.W.A., and KENDRICK, J., 2005, Molec., Phys.,
17 **103**, 719.
18
19 [21] GUEST, M.F., VAN LENTHE, J.H., KENDRICK, J., SCHOFFEL, K., and
20 SHERWOOD, P., 2005, Users Guide and Reference Manual, Version 7, Computing
21 for Science Ltd, CCLRC Daresbury Laboratory.
22
23 [22] ENGELS, G., PLESS, V., and SUTER, H.-U., 1993, Direct MRD-CI, University of
24 Bonn.
25
26 [23] KREBS, S., and BUENKER, R., 1995, J. chem. Phys., **103**, 5613.
27
28 [24] BUENKER, R.J., 1980, Proc. Workshop on Quantum Chemistry and Molecular
29 Physics, ed P.G. Burton (Australia: Wollongong).
30
31 [25] DUNNING, T.H., 1989, J. chem.. Phys., **90**, 1007.
32
33 [26] WOON, D.E., and DUNNING, T.H., 1993, J. chem.. Phys., **98**, 1358.
34
35 [27] WOON, D.E., and DUNNING, T.H., 1993, J. chem.. Phys., **100**, 2975.
36
37 [28] WILSON, A.K., WOON, D.E., PETERSON, K.A., and DUNNING, T.H., 1999, J.
38 chem. Phys., **110**, 7667.
39
40 [29] GUEST, M.F., and RODWELL, W.R., 1976, Molec. Phys., **32**, 1075.
41
42 [30] BUENKER, R.J., and PEYERIMHOFF, S.D., 1975, Chem. Phys., **8**, 56.
43
44 [31] STARACE, A.F., 1971, Phys. Rev. A., **3**, 1242.
45
46 [32] STARACE, A.F., 1973, Phys. Rev. A., **8**, 1141.
47
48 [33] VON NIESSEN, W., SCHIRMER, J., and CEDERBAUM, L.S., 1984, Comp. Phys.
49 Rep. **1**, 57.
50
51
52
53
54
55
56
57
58
59
60

- 1
2
3
4 [34] CEDERBAUM, L.S., DOMCKE, W., SCHIRMER, J., and VON NIESSEN, W.,
5
6 1986, Adv. Chem.. Phys., **65**, 115.
7
8 [35] KYDD, R.A., WIESER, H., and KIEFER, W., 1983, Spectrochim. Acta A., **39**, 173.
9
10 [36] RENNIE, E.E., COOPER, L., JOHNSON, C.A.F., PARKER, J.E., MACKIE, R.A.,
11
12 SHPINKOVA, L.G., HOLLAND D.M.P., SHAW, D.A., and HAYES, M.A., 2001,
13
14 Chem. Phys., **263**, 149.
15
16 [37] BOULANGER, A.-M., RENNIE, E.E., HOLLAND, D.M.P., SHAW, D.A., and
17
18
19
20
21
22
23
24
25
26
27
28
29
30
31
32
33
34
35
36
37
38
39
40
41
42
43
44
45
46
47
48
49
50
51
52
53
54
55
56
57
58
59
60

Table 1

Calculated transition energies, term values and oscillator strengths of valence states in trimethylene oxide.

Energy (eV)	Term value (eV)	Oscillator strength	Transitions
9.63	0.28	0.065	$3b_1 \rightarrow 17a_1(V^*)$, $3b_1 \rightarrow 4sa_1$ B ₁
9.69	2.14	0.031	$4b_2 \rightarrow 17a_1(V^*)$, $4b_2 \rightarrow 3pa_1$ B ₂
10.23	-0.32	0.000	$3b_1 \rightarrow 10b_2(V^*)$ A ₂
10.51	0.89	0.052	$8a_1 \rightarrow 17a_1(V^*)$, $8a_1 \rightarrow 4pa_1$ A ₁
10.61	1.22	0.010	$4b_2 \rightarrow 17a_1(V^*)$, $4b_2 \rightarrow 4pa_1$ B ₂
11.12	-1.21	0.001	$3b_1 \rightarrow 8b_1(V^*)$ A ₁
11.63	-1.72	0.319	$3b_1 \rightarrow 4a_2(V^*)$ B ₂
11.84	-0.44	0.075	$8a_1 \rightarrow 8b_1(V^*)$ B ₁
12.10	-0.70	0.001	$8a_1 \rightarrow 10b_2(V^*)$ B ₂
12.17	-0.77	0.013	$8a_1 \rightarrow 17a_1(V^*)$ A ₁
12.38	-2.47	0.039	$3b_1 \rightarrow 18a_1(V^*)$ B ₁
12.57	-2.66	0.006	$3b_1 \rightarrow 9b_1(V^*)$ A ₁
13.49	-1.66	0.097	$4b_2 \rightarrow 10b_2(V^*)$ A ₁
13.52	-2.12	0.096	$8a_1 \rightarrow 18a_1(V^*)$ A ₁
14.04	-2.21	0.036	$4b_2 \rightarrow 18a_1(V^*)$ B ₂

V* indicates a valence orbital

Table 2

Calculated transition energies and oscillator strengths of Rydberg states in trimethylene oxide

Energy (eV)	Oscillator strength	Transitions
7.04	0.000	$3b_1 \rightarrow 3s_{a_1}$, $3b_1 \rightarrow 3p_{a_1}$, $3b_1 \rightarrow 17a_1$ (V*) B ₁
7.42	0.006	$3b_1 \rightarrow 3p_{a_1}$, $3b_1 \rightarrow 3s_{a_1}$, $3b_1 \rightarrow 17a_1$ (V*) B ₁
7.51	0.000	$3b_1 \rightarrow 3db_2$, $3b_1 \rightarrow 3pb_2$, $3b_1 \rightarrow 4db_2$ A ₂
7.61	0.001	$3b_1 \rightarrow 3pb_1$ A ₁
8.28	0.004	$3b_1 \rightarrow 3da_1$ B ₁
8.39	0.016	$3b_1 \rightarrow 3da_2$, $3b_1 \rightarrow 4da_2$ B ₂
8.40	0.007	$3b_1 \rightarrow 3da_1$ B ₁
8.58	0.001	$3b_1 \rightarrow 3db_1$, $3b_1 \rightarrow 4db_1$, $3b_1 \rightarrow 4pb_1$ A ₁
8.62	0.000	$3b_1 \rightarrow 3db_2$, $3b_1 \rightarrow 4pb_2$, $3b_1 \rightarrow 3pb_2$ A ₂
8.93	0.010	$8a_1 \rightarrow 3p_{a_1}$, $8a_1 \rightarrow 3s_{a_1}$, $8a_1 \rightarrow 3da_1$ A ₁
8.96	0.005	$3b_1 \rightarrow 3db_1$, $3b_1 \rightarrow 4db_1$ A ₁
9.01	0.004	$3b_1 \rightarrow 4da_1$ B ₁
9.04	0.001	$3b_1 \rightarrow 3da_2$ B ₂
9.13	0.007	$8a_1 \rightarrow 3db_2$ B ₂
9.28	0.013	$8a_1 \rightarrow 3db_1$, $8a_1 \rightarrow 3pb_1$ B ₁
9.32	0.016	$8a_1 \rightarrow 3da_1$, $8a_1 \rightarrow 4s_{a_1}$, $8a_1 \rightarrow 3p_{a_1}$ A ₁
9.33	0.005	$3b_1 \rightarrow 4pb_1$ A ₁
9.87	0.019	$4b_2 \rightarrow 3db_2$ A ₁
9.90	0.003	$8a_1 \rightarrow 3da_1$ A ₁
10.04	0.004	$8a_1 \rightarrow 3da_1$, $8a_1 \rightarrow 4s_{a_1}$ A ₁
10.23	0.004	$8a_1 \rightarrow 4db_1$, $8a_1 \rightarrow 4pb_1$ B ₁
10.42	0.009	$4b_2 \rightarrow 3da_1$ B ₂
10.51	0.003	$4b_2 \rightarrow 3da_2$, $4b_2 \rightarrow 4da_2$ B ₁
10.68	0.001	$8a_1 \rightarrow 4pb_1$, $8a_1 \rightarrow 4db_1$ B ₁
10.78	0.008	$4b_2 \rightarrow 4pb_2$, $4b_2 \rightarrow 4db_2$ A ₁
10.79	0.023	$4b_2 \rightarrow 4da_1$, $8a_1 \rightarrow 4pb_2$, $8a_1 \rightarrow 4db_2$ B ₂
10.88	0.002	$8a_1 \rightarrow 4db_1$ B ₁
10.92	0.006	$8a_1 \rightarrow 4da_1$ A ₁
10.98	0.016	$2b_1 \rightarrow 3s_{a_1}$, $2b_1 \rightarrow 3da_1$ B ₁
11.02	0.006	$8a_1 \rightarrow 4s_{a_1}$ A ₁
11.07	0.001	$4b_2 \rightarrow 4da_1$ B ₂
11.08	0.008	$4b_2 \rightarrow 4da_1$, $4b_2 \rightarrow 4p_{a_1}$ B ₂
11.21	0.004	$2b_1 \rightarrow 3p_{a_1}$ B ₁
11.21	0.003	$4b_2 \rightarrow 3da_2$, $4b_2 \rightarrow 4da_2$ B ₁
11.34	0.042	$4b_2 \rightarrow 4pb_2$ A ₁
11.39	0.001	$8a_1 \rightarrow 4pb_2$, $8a_1 \rightarrow 10b_1$ (V*)
11.59	0.011	$2b_1 \rightarrow 3db_1$ A ₁
11.76	0.019	$2b_1 \rightarrow 3da_1$, $1a_2 \rightarrow 3pb_2$ B ₁
11.76	0.019	$4b_2 \rightarrow 4p_{a_1}$, $8a_1 \rightarrow 10b_2$ (V*) B ₂
12.22	0.001	$2b_1 \rightarrow 4da_1$ B ₁
12.36	0.032	$2b_1 \rightarrow 3da_1$, $2b_1 \rightarrow 4da_1$ B ₁

09-010

12.38	0.004	$2b_1 \rightarrow 4da_1 B_1$
12.47	0.023	$1a_2 \rightarrow 3db_1 B_2$
12.63	0.011	$1a_2 \rightarrow 3pb_2 B_1$
12.67	0.011	$2b_1 \rightarrow 4pb_1, 2b_1 \rightarrow 4db_1 A_1$
12.86	0.001	$2b_1 \rightarrow 4da_2 B_2$
13.11	0.033	$2b_1 \rightarrow 4pb_1 A_1$
13.18	0.002	$1a_2 \rightarrow 3da_2, 1a_2 \rightarrow 4da_2 A_1$
13.28	0.004	$1a_2 \rightarrow 4pb_1, 1a_2 \rightarrow 4db_1 B_2$
13.35	0.004	$1a_2 \rightarrow 4db_2 B_1$
13.66	0.001	$1a_2 \rightarrow 4db_2 B_1$
14.00	0.001	$1a_2 \rightarrow 4db_1 B_2$

V* indicates a valence orbital

Table 3

OVGF vertical ionization energies and charge distribution analyses in trimethylene oxide

Orbital	Ionization energy (eV)	Orbital character (% atomic population)										
		Carbon			Oxygen			Hydrogen		Rydberg		
		s	p	d	s	p	d	s	p	s	p	d
4a ₁		16.8	8.3	1.2	67.9	3.6	0.0	1.0	0.3	0.7	0.0	0.0
5a ₁		56.0	12.2	1.3	13.7	1.7	0.0	13.8	1.1	0.0	0.2	0.0
2b ₂	22.98	54.1	6.1	0.6	0.0	12.4	0.2	24.9	1.5	0.0	0.2	0.0
6a ₁	19.23	30.1	20.8	0.7	4.0	2.3	0.0	40.6	1.7	-0.1	0.0	0.0
1b ₁	17.07	0.0	51.5	0.0	0.0	18.5	0.0	23.7	0.7	0.0	0.3	0.0
7a ₁	16.55	1.3	46.5	1.3	3.9	23.6	0.1	21.4	0.7	1.1	0.0	0.0
3b ₂	15.07	0.6	49.5	1.4	0.0	44.1	0.0	3.7	0.5	0.0	0.0	0.0
1a ₂	14.38	0.0	50.8	1.1	0.0	0.0	0.0	47.2	0.7	0.0	0.0	0.0
2b ₁	13.51	0.0	36.3	1.7	0.0	22.3	0.0	39.1	0.5	0.0	0.0	0.0
4b ₂	11.83	0.2	75.5	2.2	0.0	4.6	0.0	16.6	0.7	0.0	0.0	0.0
8a ₁	11.40	0.9	39.6	1.7	2.3	45.1	0.0	9.2	0.0	0.7	0.0	0.0
3b ₁	9.91	0.0	12.1	3.0	0.0	53.6	0.0	31.3	0.2	0.0	-0.1	0.0
3s _{a1}		0.0	0.0	0.0	0.0	0.0	0.0	0.4	0.0	40.9	32.0	26.7
3p _{b2}		0.0	0.0	0.0	0.0	0.0	0.0	0.1	0.0	0.0	85.7	14.1
3p _{b1}		0.0	0.0	0.0	0.0	0.0	0.0	0.0	0.0	0.0	86.7	13.0
3p _{a1}		0.0	0.0	0.0	0.0	0.0	0.0	0.0	0.0	52.3	44.8	3.0
3d _{a1}		0.0	0.0	0.0	0.0	0.0	0.0	0.3	0.0	6.3	22.5	70.9
3d _{b2}		0.0	0.0	0.0	0.0	0.0	0.0	0.0	0.0	0.0	13.9	86.0
3d _{b1}		0.0	0.0	0.0	0.0	0.0	0.0	0.0	0.0	0.0	12.7	87.2
3d _{a2}		0.0	0.0	0.0	0.0	0.0	0.0	0.0	0.0	0.0	0.0	100.0
3d _{a1}		0.0	0.0	0.0	0.0	0.0	0.0	0.0	0.0	0.1	0.1	99.7
3s _{a1}		0.0	0.0	0.0	0.0	0.0	0.0	0.4	0.0	40.9	32.0	26.7
3p _{b2}		0.0	0.0	0.0	0.0	0.0	0.0	0.1	0.0	0.0	85.7	14.1
3p _{b1}		0.0	0.0	0.0	0.0	0.0	0.0	0.0	0.0	0.0	86.7	13.0
3p _{a1}		0.0	0.0	0.0	0.0	0.0	0.0	0.0	0.0	52.3	44.8	3.0

Table 4

Ionization energies and assignments of structure observed in the threshold photoelectron spectrum of trimethylene oxide

Assignment	Energy (eV)	Assignment	Vertical ionization energy (eV)
$(3b_1)^{-1} \tilde{X}^2B_1$ 0-0	9.679	$(8a_1)^{-1} \tilde{A}^2A_1$	11.50
5^1	9.833	$(4b_2)^{-1} \tilde{B}^2B_2$	12.17
5^2	9.989	$(2b_1)^{-1} \tilde{C}^2B_1$	13.58
$1/2^1$	10.014	$(1a_2)^{-1} \tilde{D}^2A_2$	13.98
5^3	10.146	$(3b_2)^{-1} \tilde{E}^2B_2$	15.05
$1/2^15^1$	10.179	$(7a_1)^{-1} \tilde{F}^2A_1, (1b_1)^{-1} \tilde{G}^2B_1$	16.47
$1/2^15^2$	10.343	$(6a_1)^{-1} \tilde{H}^2A_1$	18.74, 19.01

Table 5

Observed Rydberg series in trimethylene oxide converging onto the $(3b_1)^{-1} \tilde{X}^2B_1$ ionization threshold at 9.680 eV

Transition	Energy (eV)	Spacing (eV)	Assignment	Quantum defect δ	Calculated energy (eV)
$3b_1 \rightarrow nsa_1 B_1$					
n = 3	6.615		0_0^0	0.89	7.04
	6.751	0.136	5_0^1		
$3b_1 \rightarrow npa_1 B_1$					
n = 3	7.111		0_0^0	0.70	7.42
	7.264	0.153	5_0^1		
	7.418	0.307	5_0^2		
	(7.57)	(0.459)	5_0^3		
n = 4	8.62		0_0^0		
$3b_1 \rightarrow npb_1 A_1$					
n = 3	7.635	-0.019	18_2^0		
	7.654		0_0^0	0.42	7.61
	7.668	0.014	18_0^2		
	7.801	0.147	5_0^1		
	7.815	0.161	$5_0^1 18_0^2$		
n = 4	8.638		0_0^0		9.33
$3b_1 \rightarrow nda_1 B_1$					
n = 3	7.957		0_0^0	0.19	8.28
	7.967	0.010	18_0^2		
	8.103	0.146	5_0^1		
	8.113	0.156	$5_0^1 18_0^2$		
n = 4	8.711		0_0^0	0.26	9.01
	8.722	0.011	18_0^2		
	8.851	0.140	5_0^1		

1						
2						
3						
4						
5	$3b_1 \rightarrow nda_2 B_2$					
6	$n = 3$	8.003	-0.045	18_4^0		
7						
8		8.017	-0.031	$18_4^2, 18_3^1$		
9						
10		8.030	-0.018	18_2^0		
11		8.048		0_0^0	0.11	8.39
12						
13		8.061	0.013	18_0^2		
14						
15		8.173	0.125	$5_0^1 18_4^2$		
16						
17		8.208	0.160	5_0^1		
18						
19		8.218	0.170	$5_0^1 18_0^2$		
20						
21		8.362	0.314	5_0^2		
22		(8.52)	0.472	5_0^3		
23	$n = 4$					
24		8.77	-0.033	18_4^2		
25						
26		8.78	-0.023	$18_3^1, 18_2^0$		
27		8.803		0_0^0	0.07	9.04
28						
29		8.814	0.011	18_0^2		
30						
31		8.960	0.157	5_0^1		
32						
33		8.968	0.165	$5_0^1 18_0^2$		
34	$n = 5$					
35		9.119		0_0^0	0.08	
36						
37		9.129	0.010	18_0^2		
38						
39	$n = 6$					
40		9.285		0_0^0		
41						
42		9.294	0.009	18_0^2		
43						
44	$n = 7$					
45		9.390		0_0^0		
46						
47		9.401	0.011	18_0^2		
48						
49	$n = 8$					
50		9.456		0_0^0		
51						
52		9.466	0.010	18_0^2		
53						
54		9.604	0.148	5_0^1		
55	$n = 9$					
56		9.503		0_0^0		
57						
58		9.512	0.009	18_0^2		
59						
60	$n = 10$					
		9.536		0_0^0		
		9.546	0.010	18_0^2		

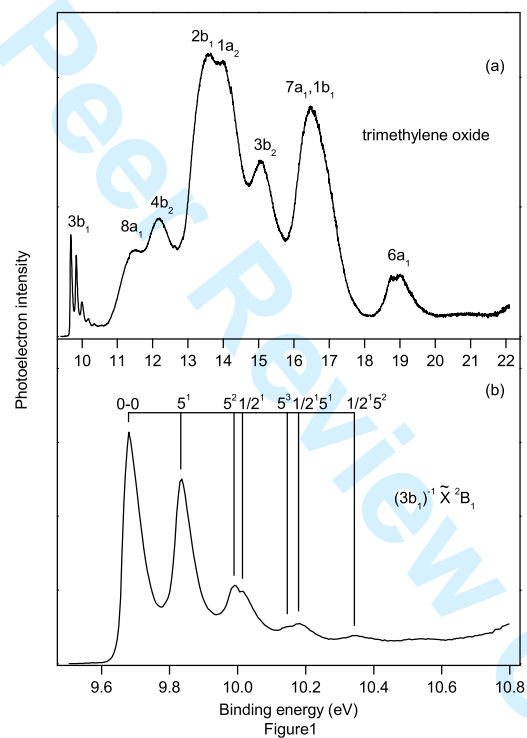
09-010

Draft 4
30-3-09

	9.687	0.151	5_0^1		
n = 11	9.557		0_0^0		
	9.567	0.010	18_0^2		
	9.71	0.153	5_0^1		
$3b_1 \rightarrow nda_1 B_1$					
n = 3	8.070		0_0^0	0.09	1.61
	8.087	0.017	18_0^2		
	8.218	0.148	5_0^1		

Figure captions

- 1
2
3
4
5
6
7
8
9
10
11
12
13
14
15
16
17
18
19
20
21
22
23
24
25
26
27
28
29
30
31
32
33
34
35
36
37
38
39
40
41
42
43
44
45
46
47
48
49
50
51
52
53
54
55
56
57
58
59
60
- Figure 1. (a) The valence shell threshold photoelectron spectrum of trimethylene oxide.
(b) The $(3b_1)^{-1} \tilde{X}^2B_1$ state threshold spectrum of trimethylene oxide showing the associated vibrational structure. Assignments and energies are given in table 4.
- Figure 2. (a) The measured absolute photoabsorption cross section of trimethylene oxide. The ionization threshold (\tilde{X}^2B_1) is marked. (b) The calculated oscillator strengths for transitions into Rydberg states. Assignments are given in table 2.
(c) The calculated oscillator strengths for transitions into excited valence states. Assignments are given in table 1.
- Figure 3. The absolute photoabsorption cross section of trimethylene oxide between 5.9 and 8.0 eV showing structure due to excitation of an electron from the $3b_1$ orbital. Assignments and energies are given in table 5.
- Figure 4. The absolute photoabsorption cross section of trimethylene oxide between 7.7 and 8.8 eV showing structure due to excitation of an electron from the $3b_1$ orbital. Assignments and energies are given in table 5.
- Figure 5. The absolute photoabsorption cross section of trimethylene oxide between 8.7 and 9.9 eV showing structure due to excitation of an electron from the $3b_1$ orbital. Assignments and energies are given in table 5.
- Figure 6. The photoabsorption spectra of trimethylene sulphide, ethylene sulphide, trimethylene oxide and ethylene oxide in the energy range below their ionization thresholds, to highlight the Rydberg structure due to excitation from the outermost orbital. The correlation amongst related structure is indicated by dotted lines.



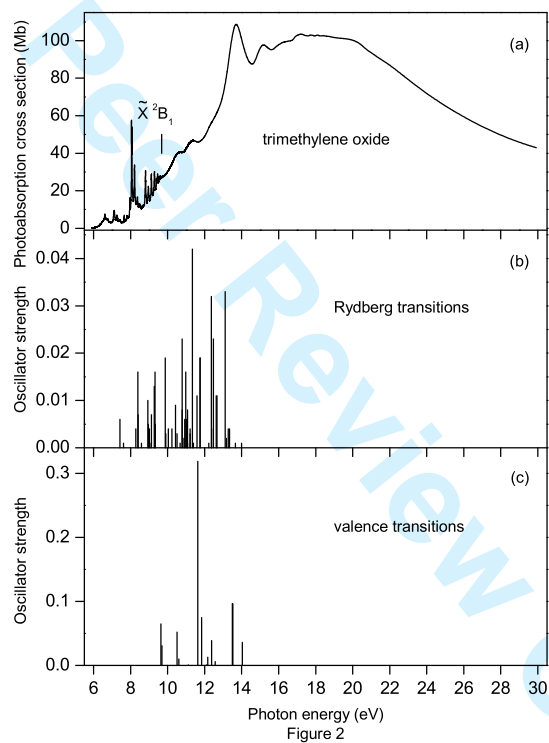
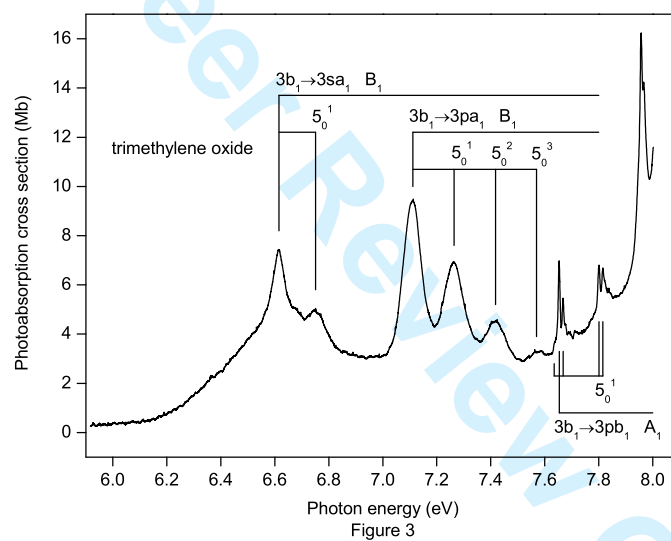
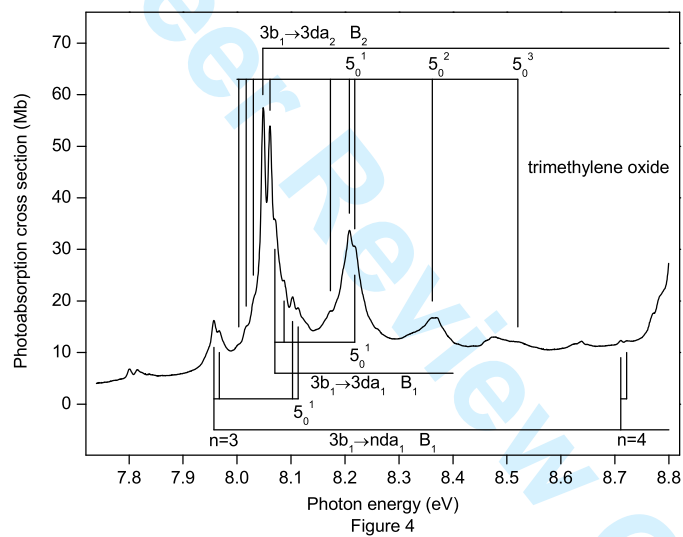


Figure 2





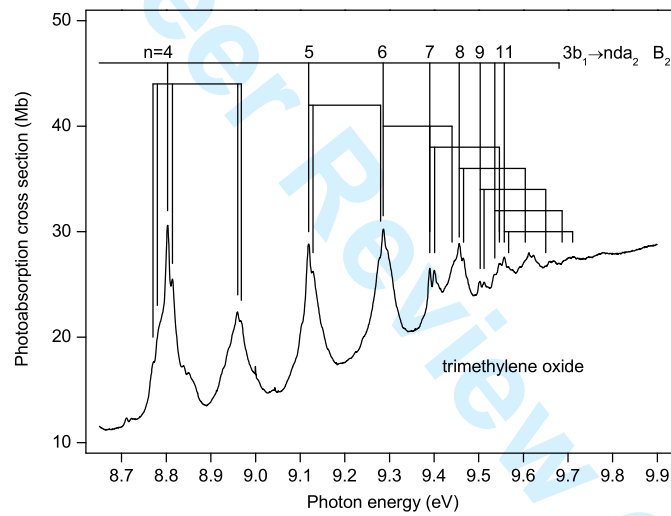


Figure 5

